# On the Influence of Geometry on Optimized Schwarz Methods

Martin J. Gander*

October 7, 2010

**Abstract**

The convergence of Schwarz methods can be influenced by the geometry of the decomposition, and therefore also the optimized parameters in optimized Schwarz methods depend on the geometry. We present a first study of this influence, which reveals that in contrast to results in the literature so far, where only the interface length is taken into account, the diameter of the subdomains can play an important role as well. The new estimate also includes the influence of lateral boundary conditions.

## 1 Introduction

Schwarz domain decomposition methods are the oldest domain decomposition methods we know; they were invented by Herman Amandus Schwarz in 1869, see [10], in order to prove rigorously the Dirichlet principle, which lies at the heart of Riemann's theory of analytic functions. For more historical background on continuous and discrete Schwarz methods, see the historical review paper [4], and for the analysis of classical Schwarz methods, see the books [11, 9, 12]. More recently, optimized Schwarz methods have been developed, see the pioneering work in [6, 7, 1], and [3] and references therein. These methods use more effective transmission conditions, which are based on approximations of the Dirichlet to Neumann map at the interfaces between subdomains. In order to get the best performance in a class of approximations, an optimization problem needs to be solved, such that the convergence factor of the associated method is minimized, which implies that the convergence rate is maximized. Since these optimized transmission conditions depend on the underlying PDE, the optimized parameters will also depend on the PDE, and usually a model problem with a decomposition into two half spaces is used, together with Fourier analysis, in order to determine a physically relevant convergence factor for a given problem, which is then minimized. Using asymptotic analysis when the mesh parameter gets small, often one can get explicit asymptotic formulas for the optimized

*Mathematics Section, University of Geneva, CH-1211, Geneva, Switzerland

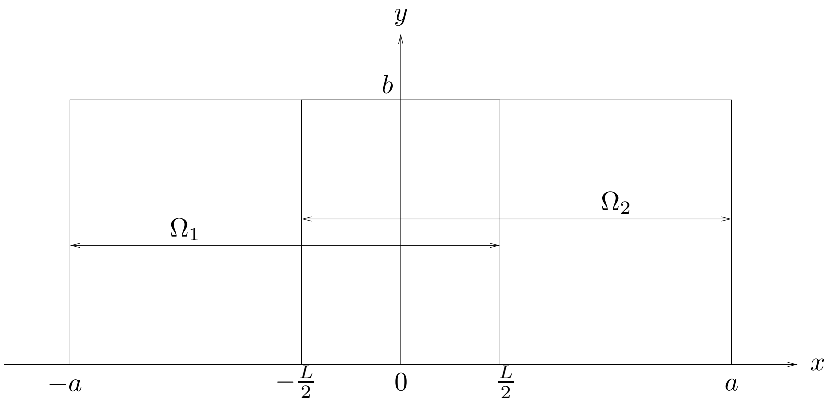


Figure 1: Geometry of the domain decomposition used

parameters, which depend on the physical parameters in the underlying PDE, but because of the half space decomposition, the information of the geometry of the decomposition is lost. So far the only reintroduction of geometry is based on the estimation of a minimum relevant frequency, which introduces the length of the interface, see for example [3]. A related problem is that these estimates assume lateral Dirichlet conditions at the end of the interfaces, which is often not the case. Several numerical experiments in different contexts, for example the use of optimized Schwarz waveform relaxation methods [5], or the heating of an apartment, simulated by a classical and optimized Schwarz method [8], have shown that while the asymptotic scaling of the optimized parameters is indeed optimal, the constant in front can often be modified by a factor of order one to get still faster numerical convergence. The purpose of this short note is to analyze in detail a classical and optimized overlapping Schwarz method for a model problem on a bounded domain with specific geometric parameters, in order to study their influence on the optimized parameters and convergence rate of the underlying methods. For the non-overlapping case, see [2].

# 2 The Model Problem

We propose to study the model problem of the Poisson equation

$$\begin{aligned} \Delta u &= f && \text{in } \Omega := (-a,a)\times(0,b), \\ u(-a,y)=u(a,y) &= 0 && y\in(0,b), \\ \mathcal{B}(u)(x,0)=\mathcal{B}(u)(x,b) &= 0 && x\in(-a,a). \end{aligned} \tag{1}$$

Here $\mathcal{B}$ will either be a Dirichlet boundary condition, $\mathcal{B}=I$, or a Neumann boundary conditions, $\mathcal{B}=\partial_y$. We decompose the domain $\Omega$ into two overlapping subdomains $\Omega_1 := (-a,\frac{L}{2})\times(0,b)$ and $\Omega_2 := (-\frac{L}{2},a)\times(0,b)$, $L>0$, as shown in Figure 1, and will study the corresponding Schwarz algorithm

$$
\begin{array}{rcll}
\Delta u_1^n & = & f & \text{in } \Omega_1, \\
\mathcal{B}(u)(x,0) = \mathcal{B}(u)(x,b) & = & 0 & x \in (-a, \frac{L}{2}), \\
u_1^n(-a,y) & = & 0 & y \in (0,b), \\
\mathcal{B}_1(u_1^n)(\frac{L}{2},y) & = & \mathcal{B}_1(u_2^{n-1})(\frac{L}{2},y) & y \in (0,b), \\
\Delta u_2^n & = & f & \text{in } \Omega_2, \\
\mathcal{B}(u)(x,0) = \mathcal{B}(u)(x,b) & = & 0 & x \in (-\frac{L}{2}, a), \\
u_2^n(a,y) & = & 0 & y \in (0,b), \\
\mathcal{B}_2(u_2^n)(-\frac{L}{2},y) & = & \mathcal{B}_2(u_1^{n-1})(-\frac{L}{2},y) & y \in (0,b),
\end{array} \tag{2}
$$

where the transmission operators are either of Dirichlet type, $\mathcal{B}_j = I$, $j = 1, 2$, in order to obtain a classical Schwarz method, or of Robin type, $\mathcal{B}_j = \partial_x \pm p$, $j = 1, 2$, $p > 0$, to obtain an optimized Schwarz method. In this simple geometric setting, the complete analysis of the algorithms using sine and cosine expansions is possible, and will reveal the influence of the geometry on the convergence of the algorithms.

# 3 Analysis of the Classical Schwarz Method

We expand the iterates $u_j^n$, $j = 1, 2$ of algorithm (2) into a sine or cosine series, depending on the Dirichlet or Neumann boundary condition on top and at the bottom,

$$
u_j^n(x,y) = \begin{cases} \displaystyle\sum_{k=1}^{\infty} \hat{u}_j^n(x,k) \sin(\tfrac{k\pi}{b} y), & \text{if } \mathcal{B} = I, \\ \displaystyle\sum_{k=0}^{\infty} \hat{u}_j^n(x,k) \cos(\tfrac{k\pi}{b} y), & \text{if } \mathcal{B} = \partial_y. \end{cases} \tag{3}
$$

This guarantees that the homogeneous top and bottom boundary conditions are satisfied. In order to study the convergence factor, it suffices by linearity to study the homogeneous version of (2), and we set from now on $f := 0$ in what follows. Inserting the expansions (3) into the equations (2) defining the algorithm, we obtain the equation

$$
\partial_{xx} \hat{u}_j^n(x,k) - \left(\tfrac{k\pi}{b}\right)^2 \hat{u}_j^n(x,k) = 0, \quad j = 1, 2, \tag{4}
$$

and thus the series coefficients for $k = 1, 2, \ldots$ are given by

$$
\begin{array}{rcl}
\hat{u}_1^n(x,k) & = & A_1^n(k) \sinh(\frac{k\pi}{b}(x+a)), \\
\hat{u}_2^n(x,k) & = & A_2^n(k) \sinh(\frac{k\pi}{b}(x-a)),
\end{array} \tag{5}
$$

where we used the homogeneous Dirichlet conditions on the left and right. In the case of the cosine series, we also need to solve equation (4) for $k = 0$, which leads to the linear solutions

$$
\begin{array}{rcl}
\hat{u}_1^n(x,0) & = & A_1^n(0)(a+x), \\
\hat{u}_2^n(x,0) & = & A_2^n(0)(a-x).
\end{array} \tag{6}
$$

The remaining constants $A_j^n$, $j = 1, 2$ in these iterates are determined by the transmission conditions in algorithm (2), and in the case of the classical Schwarz method, they are Dirichlet conditions. Inserting the solution of subdomain $\Omega_2$, evaluated at $x = \frac{L}{2}$, into the transmission condition of subdomain $\Omega_1$, we find for the constant at iteration step $n+1$ on $\Omega_1$,

$$A_1^{n+1}(k) = \begin{cases} \frac{\sinh(\frac{k\pi}{b}(\frac{L}{2}-a))}{\sinh(\frac{k\pi}{b}(\frac{L}{2}+a))} A_2^n(k), & k = 1, 2, \ldots \\ \frac{\frac{L}{2}-a}{\frac{L}{2}+a} A_2^n(k), & k = 0. \end{cases}$$

Inserting the solution of subdomain $\Omega_1$, evaluated at $x = -\frac{L}{2}$, into the transmission condition of subdomain $\Omega_2$, we find for the constant at iteration step $n$ on $\Omega_2$,

$$A_2^n(k) = \begin{cases} \frac{\sinh(\frac{k\pi}{b}(-\frac{L}{2}+a))}{\sinh(\frac{k\pi}{b}(-\frac{L}{2}-a))} A_1^{n-1}(k), & k = 1, 2, \ldots \\ \frac{-\frac{L}{2}+a}{-\frac{L}{2}-a} A_1^{n-1}(k), & k = 0. \end{cases}$$

Combining the two, we obtain the convergence factor of the classical Schwarz method,

$$\rho_{cla}(k, a, b, L) := \sqrt{\frac{A_1^{n+1}(k)}{A_1^{n-1}(k)}} = \begin{cases} \frac{\sinh(\frac{k\pi}{b}(a-\frac{L}{2}))}{\sinh(\frac{k\pi}{b}(a+\frac{L}{2}))}, & k = 1, 2, \ldots \\ \frac{a-\frac{L}{2}}{a+\frac{L}{2}}, & k = 0. \end{cases} \tag{7}$$

Denoting by $||u(\cdot, \cdot)||_{\infty,2}$ the infinity norm in $x$, and the spectral norm in $y$, we obtain:

**Proposition 3.1** *The classical Schwarz method, (2) with $\mathcal{B} = I$, converges geometrically for both Dirichlet and Neumann conditions on the top and at the bottom (see Figure 1). The errors in the iteration satisfy for $n$ even*

$$||u_j^n(\cdot, \cdot)||_{\infty,2} \leq R_{cla}^n ||u_j^0(\cdot, \cdot)||_{\infty,2}, \quad 0 < R_{cla} < 1. \tag{8}$$

*When the overlap $L$ goes to zero, we have*

$$R_{cla} = \begin{cases} 1 - \frac{\pi}{b\tanh(\frac{a\pi}{b})} L + O(L^2), & \textit{Dirichlet conditions,} \\ 1 - \frac{1}{a} L + O(L^2), & \textit{Neumann conditions.} \end{cases} \tag{9}$$

**Proof** Letting $R_{cla} := \max_k |\rho_{cla}(k, a, b, L)|$, we obtain $0 < R_{cla} < 1$, and using Parseval's Theorem, we have ($+$ corresponds to $j = 1$ and $-$ to $j = 2$)

$$\begin{aligned} ||u_j^n(\pm\frac{L}{2}, \cdot)||_2^2 &= \sum_k (A_1^n(k) \sinh(\frac{k\pi}{b}(a \pm \frac{L}{2})))^2 \\ &= \sum_k ((\rho_{cla}(k, a, b, L))^2 A_j^{n-2}(k) \sinh(\frac{k\pi}{b}(a \pm \frac{L}{2})))^2 \\ &\leq R_{cla}^4 \sum_k (A_j^{n-2}(k) \sinh(\frac{k\pi}{b}(a \pm \frac{L}{2})))^2 \\ &= R_{cla}^4 ||u_j^{n-2}(\pm\frac{L}{2}, \cdot)||_2^2. \end{aligned}$$

Now using the maximum principle, we obtain

$$||u_j^n(\cdot,\cdot)||_{\infty,2} = R_{cla}^2 ||u_j^{n-2}(\cdot,\cdot)||_{\infty,2},$$

and thus the first result (8) follows by induction.

In order to prove the second result (9), we note that the convergence factor in (7) is biggest for $k = 0$ in the case of Neumann conditions, and $k = 1$ for Dirichlet conditions. Hence it suffices to expand $\rho_{cla}(0, a, b, L)$ and $\rho_{cla}(1, a, b, L)$ for $L$ small, to obtain (9). ∎

Expanding the leading coefficent in the case of Dirichlet conditions in (9) for $a$ small or $b$ large, we get

$$\frac{\pi}{b\tanh(\frac{a\pi}{b})} = \frac{1}{a} + \frac{\pi^2}{3}\frac{a}{b^2} + O(\frac{a^3}{b^4}),$$

which shows that the method with Dirichlet conditions converges faster than with Neumann conditions. We also see that large $a$ slows down the convergence in both cases.

The analysis in [3], which was based on two half space problems and the estimate $\frac{\pi}{b}$ for the lowest frequency along the interface, gave

$$\tilde{R}_{cla} = e^{-\frac{\pi}{b}L} = 1 - \frac{\pi}{b}L + O(L^2).$$

We see that this analysis can not reflect the influence of the bounded domain in the $x$ direction. It however corresponds to the case of Dirichlet conditions below and above when $a$ goes to infinity, as one can see from (9). For the particular domain where $b = a\pi$, the old result also coincides with the new result for Neumann conditions below and above.

# 4 Analysis of the Optimized Schwarz Method

We now study the optimized Schwarz method, algorithm (2) with $\mathcal{B}_j = \partial_x \pm p$, $j = 1, 2$, $p > 0$. The expansions for the subdomain solutions remain the same, up to equation (6), only once one uses the transmission conditions the situation changes. Inserting the solution of subdomain $\Omega_2$, evaluated at $x = \frac{L}{2}$, into the transmission condition of subdomain $\Omega_1$, we find now for the constant at iteration step $n + 1$ on $\Omega_1$,

$$A_1^{n+1}(k) = \begin{cases} \frac{\frac{k\pi}{b}\cosh(\frac{k\pi}{b}(\frac{L}{2}-a))+p\sinh(\frac{k\pi}{b}(\frac{L}{2}-a))}{\frac{k\pi}{b}\cosh(\frac{k\pi}{b}(\frac{L}{2}+a))+p\sinh(\frac{k\pi}{b}(\frac{L}{2}+a))} A_2^n(k), & k = 1, 2, \ldots \\ \frac{1+p(\frac{L}{2}-a)}{1+p(\frac{L}{2}+a)} A_2^n(k), & k = 0. \end{cases}$$

Inserting the solution of subdomain $\Omega_1$, evaluated at $x = -\frac{L}{2}$, into the transmission condition of subdomain $\Omega_2$, we find for the constant at iteration step $n$ on $\Omega_2$,

$$A_2^n(k) = \begin{cases} \frac{\frac{k\pi}{b}\cosh(\frac{k\pi}{b}(-\frac{L}{2}+a))-p\sinh(\frac{k\pi}{b}(-\frac{L}{2}+a))}{\frac{k\pi}{b}\cosh(\frac{k\pi}{b}(-\frac{L}{2}-a))-p\sinh(\frac{k\pi}{b}(-\frac{L}{2}-a))} A_1^{n-1}(k), & k = 1, 2, \ldots \\ \frac{1-p(-\frac{L}{2}+a)}{1-p(-\frac{L}{2}-a)} A_1^{n-1}(k), & k = 0. \end{cases}$$

Combining again both steps, we obtain the convergence factor of the optimized Schwarz method,

$$\rho_{opt}(k,a,b,L,p) = \begin{cases} \frac{\frac{k\pi}{b}\cosh(\frac{k\pi}{b}(a-\frac{L}{2}))-p\sinh(\frac{k\pi}{b}(a-\frac{L}{2}))}{\frac{k\pi}{b}\cosh(\frac{k\pi}{b}(a+\frac{L}{2}))+p\sinh(\frac{k\pi}{b}(\frac{L}{2}+a))}, & k=1,2,\ldots \\ \frac{1-p(a-\frac{L}{2})}{1+p(a+\frac{L}{2})}, & k=0. \end{cases} \quad (10)$$

**Proposition 4.1** *The optimized Schwarz method, (2) with $\mathcal{B} = \partial_x \pm p$, $p \geq 0$, converges geometrically for both Dirichlet and Neumann conditions on the top and at the bottom (see Figure 1). The errors in the iteration satisfy for $n$ even*

$$||u_j^n(\cdot,\cdot)||_{\infty,2} \leq (R_{opt}(p))^n ||u_j^0(\cdot,\cdot)||_{\infty,2}, \quad 0 < R_{opt}(p) < 1. \quad (11)$$

**Proof** We first show that the convergence factor given in (10) is smaller than one in modulus for all $p$ and $k$. This convergence factor is for both $k > 0$ and $k = 0$ of the form

$$\frac{\alpha - p\beta}{\gamma + p\delta}, \quad \alpha,\beta,\gamma,\delta > 0,$$

with $\alpha < \gamma$ and $\beta < \delta$. We then have, since also $p \geq 0$,

$$|\frac{\alpha - p\beta}{\gamma + p\delta}| < 1 \Longleftrightarrow |\alpha - p\beta| < \gamma + p\delta \Longleftrightarrow -\gamma - p\delta < \alpha - p\beta < \gamma + p\delta.$$

Now the first inequality holds, since

$$-\gamma - \alpha < p(\delta - \beta),$$

because $\delta > \beta$, and the second inequality holds, since

$$\alpha - \gamma < p(\beta + \delta),$$

because $\gamma > \alpha$. Since in addition $\rho_{opt}(k,a,b,L,p)$ goes to zero when $k$ goes to infinity we have that $R_{opt}(p) := \sup_k |\rho_{opt}(k,a,b,L,p)|$ satisfies $0 < R_{opt}(p) < 1$. We can now apply Parseval's Theorem, and the maximum principle, as in the first part of the proof of Proposition 3.1, to conclude the proof. ∎

**Proposition 4.2** *The optimal choice for the parameter $p$ in the optimized Schwarz method, (2) with $\mathcal{B} = \partial_x \pm p$, is for small overlap $L$ given by*

$$p^* = \begin{cases} \left(\frac{\pi^2}{2b^2\tanh^2(\frac{\pi a}{b})}\right)^{\frac{1}{3}} L^{-\frac{1}{3}}, & \textit{Dirichlet conditions}, \\ (\frac{1}{2a^2})^{\frac{1}{3}} L^{-\frac{1}{3}}, & \textit{Neumann conditions}, \end{cases} \quad (12)$$

*and the corresponding convergence factors are*

$$R_{opt} = \begin{cases} 1 - 2\left(\frac{2\pi}{b\tanh(\frac{\pi a}{b})}\right)^{\frac{1}{3}} L^{\frac{1}{3}} + O(L^{\frac{2}{3}}), & \textit{Dirichlet conditions}, \\ 1 - 2\left(\frac{2}{a}\right)^{\frac{1}{3}} L^{\frac{1}{3}} + O(L^{\frac{2}{3}}), & \textit{Neumann conditions}. \end{cases} \quad (13)$$

**Proof** We start by studying the case of Dirichlet conditions, $k \geq 1$. We first note that $\rho_{opt}$ in (10) goes to zero as $k$ goes to infinity, and for $p = 0$, the convergence factor $\rho_{opt}$ is non-negative for all $k$. Now the partial derivative of $\rho_{opt}$ with respect to $p$ shows that $\rho_{opt}$ is decreasing when $p$ increases, for all $k$. Hence increasing $p$ starting from zero decreases the maximum of the convergence factor. However, for any given $k$, we see from (10) that $\rho_{opt}$ remains non-negative for all $p \in [0, \bar{p}(k)]$, with

$$\bar{p}(k) = \frac{k\pi}{b\tanh(\frac{k\pi}{b(a-\frac{L}{2})})}. \tag{14}$$

In particular when $p$ becomes bigger than $\bar{p}(1)$, we have $\rho_{opt}(1, a, b, L, p) < 0$, and for p large, we obtain

$$\rho_{opt}(1, a, b, L, p) = -\frac{\sinh(\frac{k\pi}{b}(a - \frac{L}{2}))}{\sinh(\frac{k\pi}{b}(a + \frac{L}{2}))} + O(\frac{1}{p}),$$

which shows that for $L$ small, $\rho_{opt}(1, a, b, L, p)$ will approach $-1$. We now study the partial derivative of $\rho_{opt}$ with respect to $k$, and find that for $L$ small, there is only one extremum, a maximum, at

$$\bar{k}(p) = \frac{b\sqrt{Lp(Lp+2)}}{\pi L}.$$

The optimum choice $p^*$ for $L$ small is therefore by continuity given by the equioscillation condition

$$\rho_{opt}(1, a, b, L, p^*) + \rho_{opt}(\bar{k}(p^*), a, b, L, p^*) = 0.$$

Solving this equation for $L$ small leads to the result stated in equation (12) for the Dirichlet case.

The analysis for the Neumann case is similar, the only difference is that now the role of $\rho_{opt}(1, a, b, L, p^*)$ is played by $\rho_{opt}(0, a, b, L, p^*)$, and the equioscillation condition is

$$\rho_{opt}(0, a, b, L, p^*) + \rho_{opt}(\bar{k}(p^*), a, b, L, p^*) = 0,$$

which leads, after solving for $L$ small to the result stated in equation (12) for the Neumann case. ■

The analysis in [3], which was based on two half space problems and the estimate $\frac{\pi}{b}$ for the lowest frequency along the interface, gave for the optimized parameter

$$\tilde{p}^* = \left(\frac{\pi^2}{2b^2}\right)^{\frac{1}{3}} L^{-\frac{1}{3}}.$$

Again, we see that this analysis can not reflect the influence of the bounded domain in the $x$ direction. This old result corresponds to the new analysis with Dirichlet conditions below and above, when $a$ goes to infinity. But like in the case of the classical Schwarz method, for the particular domain where $b = a\pi$, the old result obtained with an estimate based on Dirichlet conditions below and above coincides with the new result for Neumann conditions.

## 5 Conclusion

We have given convergence estimates and asymptotic formulas for optimized Schwarz methods applied to the Poisson problem on bounded domains in the case where the original problem has Dirichlet or Neumann boundary conditions where the interface touches the boundary. We compared our results with the estimates obtained from a simpler Fourier analysis on unbounded domains from the literature, and found the new result that the domain diameter can be relevant for determining the optimized parameter.

## References


[1] Philippe Chevalier and Frédéric Nataf. Symmetrized method with optimized second-order conditions for the Helmholtz equation. In *Domain decomposition methods, 10 (Boulder, CO, 1997)*, pages 400–407. Amer. Math. Soc., Providence, RI, 1998.

[2] Ibrahima Cisse. *Méthodes de décomposition de domaines pour des structures hétérogènes.* PhD thesis, Université Paris 13, 2009.

[3] Martin J. Gander. Optimized Schwarz methods. *SIAM J. Numer. Anal.*, 44(2):699–731, 2006.

[4] Martin J. Gander. Schwarz methods over the course of time. *Electronic Transactions on Numerical Analysis*, 31:228–255, 2008.

[5] Loic Gouarin and Caroline Japhet. Personal Communication.

[6] Caroline Japhet. Optimized Krylov-Ventcell method. Application to convection-diffusion problems. In Petter E. Bjørstad, Magne S. Espedal, and David E. Keyes, editors, *Proceedings of the 9th international conference on domain decomposition methods*, pages 382–389. ddm.org, 1998.

[7] Caroline Japhet, Frédéric Nataf, and Francois-Xavier Roux. The Optimized Order 2 Method with a coarse grid preconditioner. application to convection-diffusion problems. In P. Bjorstad, M. Espedal, and D. Keyes, editors, *Ninth International Conference on Domain Decompositon Methods in Science and Engineering*, pages 382–389. John Wiley & Sons, 1998.

[8] Felix Kwok. Personal Communication.

[9] Alfio Quarteroni and Alberto Valli. *Domain Decomposition Methods for Partial Differential Equations.* Oxford Science Publications, 1999.

[10] H. A. Schwarz. Über einen Grenzübergang durch alternierendes Verfahren. *Vierteljahrsschrift der Naturforschenden Gesellschaft in Zürich*, 15:272–286, May 1870.

[11] Barry F. Smith, Petter E. Bjørstad, and William Gropp. *Domain Decomposition: Parallel Multilevel Methods for Elliptic Partial Differential Equations.* Cambridge University Press, 1996.

[12] Andrea Toselli and Olof Widlund. *Domain Decomposition Methods - Algorithms and Theory*, volume 34 of *Springer Series in Computational Mathematics.* Springer, 2004.